35th Annual International Conference of the IEEE EMBS
Osaka, Japan, 3 - 7 July, 2013

Depth Estimation and Image Improvement of Fluorescent Objects in Scattering Medium with Unknown Optical Parameters *

Jiao Xia, Takeshi Namita, *Member*, *IEEE*, Yuji Kato, and Koichi Shimizu, *Senior Member*, *IEEE*

***Abstract*—The depth of fluorescent source is required to suppress the scattering effect in transcutaneous fluorescent imaging. We have developed a technique to estimate the depth using two light sources. However, with this technique, the reduced scattering coefficient (μ_s') and the absorption coefficient (μ_a) of the scattering medium have to be known a priori. To eliminate this requirement, we devised a technique that uses three excitation sources. The feasibility of the proposed technique was verified in both computer simulation and experiment. It was demonstrated that we could estimate the depth of the fluorescent source and improve the fluorescent image even with μ_s' and μ_a variation.**

I. Introduction

The importance of transcutaneous fluorescent imaging (TFI) in research and clinical practice has been widely recognized. TFI of lymph vessels and lymph nodes with indocyanine green (ICG) has been used in clinical practice. TFI with ICG has also been used in the diagnosis and therapy of skin cancer, breast cancer and rectal cancer [1]. However, due to the scattering effect of tissue, the TFI image is greatly blurred and the identification of the true distribution of the fluorescent source in the turbid medium is difficult. To make the TFI method more practical, a technique to suppress the scattering effect by the deconvolution with the point spread function (PSF) was developed. The applicability and effectiveness of this technique were confirmed in animal experiments [2]. This PSF was given as a function of the depth of the fluorescent source and optical parameters of the turbid medium. In the equation of this PSF, the depth is the most dominant factor to determine the spread of the PSF. Therefore, the depth of the fluorescent source has to be estimated for clear TFI. If we can estimate an appropriate depth of the fluorescent source, we can expect to recover the image of a relatively small (less than a few centimeter) and discrete fluorescent object at the depth less than a few centimeter depth with a few millimeter spatial resolution.

For this purpose, we developed a technique to estimate the depth of a fluorescent source using two excitation sources at the different positions along the surface with the known optical coefficients of the turbid medium [3]. For the accurate estimation in this technique, the reduced scattering coefficient (μ_s') and the absorption coefficient (μ_a) of the turbid medium were required. To overcome this difficulty and to make this technique more practical, a new technique was developed and the feasibility was examined in computer simulation and experiment.

* A part of this research was supported by a Grant-in-Aid for Scientific Research from the Japan Society for the Promotion of Science.

X. Jiao (phone: +81-11-706-7229; fax: +81-11-706-7219; jiaoxia @bme.ist.hokudai.ac.jp), T. Namita (tnamita@bme.ist.hokudai.ac.jp), Y. Kato (kato@bme.ist.hokudai.ac.jp), and K. Shimizu (shimizu@bme. ist.hokudai.ac.jp) are with the Graduate School of Information Science and Technology, Hokkaido University, N14, W9, Kita-ku, Sapporo 060-0814 JAPAN

II. Basic Principle of Depth Estimation

Fig. 1 depicts the original principle of the depth estimation. Excitation light is illuminated on the body surface using two emitters at different distances from the center of the observation area. The variables l and I are the distance from the emitter to the fluorescent object and the observed intensity at the body surface, respectively. The subscripts, S and L correspond to the excitation with the emitters at the small and the large distances, respectively. For example, I_S indicates the fluorescent intensity reached to the body surface when the fluorescent object is illuminated with the excitation source at the distance l_S.

It can be seen that in Fig. 1 that the ratio l_S/l_L is monotonically dependent on the depth of the fluorescent object. The more the ratio approaches to 1 for the deeper fluorescent object. The intensity of the excitation light at the fluorescent object and that of the fluorescent light at the body surface is strongly dependent on the distance l. Therefore, the ratio I_S/I_L is also dependent on the depth and approaches to 1 for the deeper object. This suggests the possibility to estimate the depth from the fluorescent intensity captured by the CCD camera at the body surface using the two emitters at different distances from the observation area.

In the estimation process, we obtain a calibration curve first either in simulation or phantom measurement. Fig. 2 shows a typical example of the calibration curve obtained in an experiment. Then we illuminate the object using the ring-emitters with different diameters, and measure the fluorescent intensity I_S and I_L at the body surface. From the value I_S/I_L, we can estimate the depth of the fluorescent object using the calibration curve.

The effectiveness of the depth estimation from the calibration curve was confirmed in experiments [3]. In these experiments, it was also found that the calibration curve was dependent on the optical parameters, or μ_s' and μ_a. Therefore, in this technique, we have to know the optical parameters to obtain an appropriate calibration curve either in the simulation or the experiment with a model phantom.

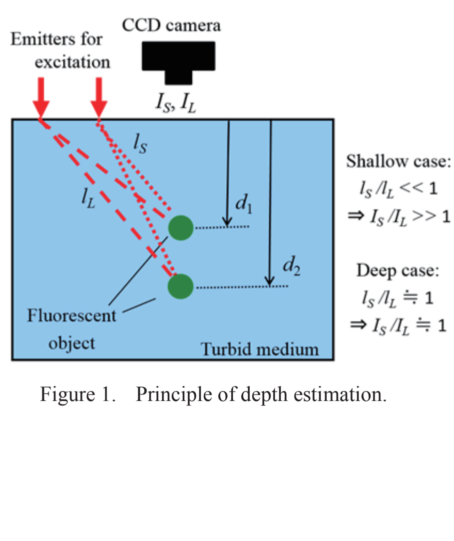

Figure 1. Principle of depth estimation.

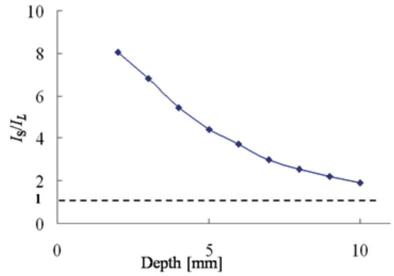

Figure 2. Typical example of calibration curve for depth estimation using measured fluorescent intensity ratio.

III. Depth Estimation with an Unknown Optical Parameter

A. Principle of Proposed Technique

The required parameters, μ_s' and μ_a of the turbid medium can be measured or estimated with various techniques. It would be better, however, if we can estimate them at the same time as the object depth using the same arrangement of the measurement. To answer this requirement, we modified the above principle. We added another emitter of excitation light between the two emitters. The distance and the observed intensity of this emitter are denoted as l_M and I_M, respectively.

Using the fluorescent intensity I_M, we draw the calibration curve of I_L/I_M versus I_M/I_S for vertical and horizontal axes, respectively. In simulation or a phantom measurement, this curve is obtained as a function of the unknown optical parameter, such as μ_a in the case of constant μ_s'. When the depth of the fluorescent object changes, the curve shifts parallel. Therefore, we draw the curves for many different depths as calibration curves. In the depth estimation, we measure I_S, I_M and I_L. And we find the measured point in I_L/I_M - I_M/I_S plane. Then, we can identify the specific curve which passes this point, and we can estimate the depth from the shift of the specific curve. Since this calibration curve is a function of μ_a, we do not need the value of μ_a a priori. In addition, we can estimate the unknown parameter μ_a at the same time.

B. Feasibility Check in Simulation

To test the feasibility of the above principle, we generated calibration curves in computer simulation. The radii of the three ring-emitters were 15, 20 and 25 mm, respectively. As a fluorescent object, a thin fluorescent plate of square shape (2×2 mm^2) was placed in a scattering medium with the flat face toward the body surface. The depth was set at 3, 5, 7 and 10 mm. The optical constants of scattering medium was set in the range μ_s' = 0.5–1.5 /mm and μ_a = 0.005–0.015 /mm. Typical example of the calibration curves are shown in Fig. 3. I_L, I_M and I_S are shown as I (25mm), I (20mm) and I (15mm), respectively. Small circles on the calibration curve show the points with different μ_a and μ_s' in Figs. 3(a) and 3(b), respectively. The known optical parameter was μ_s'= 1.0 /mm and μ_a=0.01 /mm in Figs. 3(a) and 3(b), respectively.

The calibration curve was obtained as a function of the unknown optical parameter, and its shift corresponded to the depth of the fluorescent object. The amount of the shift is monotonically dependent on the depth, and we can estimate the depth value as a weighted average of the two shifts which hold the measurement point in between. The result of this analysis verified the feasibility of the proposed technique.

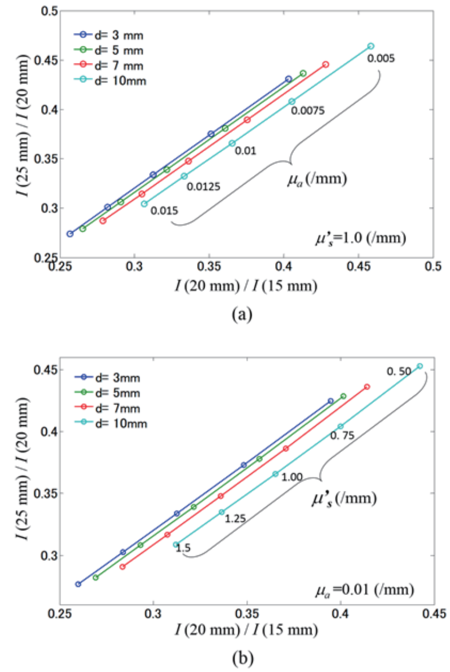

Figure 3. Calibration curves obtained in simulation (a) μ_s' is fixed to 1.0 /mm (b) μ_a is fixed to 0.01 /mm.

C. Experimental Verification

We tested the effectiveness of this technique in an experiment. Fig. 4 shows the experiment setup. Excitation light from a laser (Ti:Sapphire, 765 nm wavelength) was guided to the surface of a scattering medium by an optical fiber. To simulate the condition of the three emitters, the end of the fiber was set 15, 20 and 25 mm from the center of the fluorescent object. The fluorescent image was taken with the cooled CCD camera through a band-pass filter (830 nm, 10 nm FWHM). Intensity was calculated from the integration of the image data. As a fluorescent object, ICG was mixed in the epoxy resin in the shape of rectangular parallel piped (2×2×0.6 mm^3). It was placed in a scattering medium (Intralipid suspension) at the depth 3, 5, 7, and 10 mm using thin transparent plates. The scattering coefficient of the medium was μ_s' = 1.0 /mm and the absorption coefficient was varied in the range μ_a = 0.005–0.015 /mm.

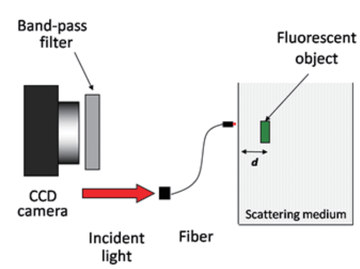

Figure 4. Experiment setup.

The measured calibration curves were shown in Fig. 5. The general characteristics of the calibration curve agreed well with those of the simulation. With these calibration curves, the depth estimation was attempted. Using the same fluorescent object at 4, 6 and 8 mm depth. The measured points were shown in Fig. 5 as I, II and III. The depths estimated from calibration curves are summarized in Table 1. The estimated depth agreed well with the given depth within 6% error.

Table 1. Results of depth estimation.

Given depth [mm]	Estimated depth [mm]	Depth Estimation error [%]
4.0	4.11	2.6
6.0	6.29	4.8
8.0	7.54	5.8

As mentioned above, the value of μ_a can be estimated in the same process. The estimated values for I, II and III were summarized in Table 2. The estimated μ_a agreed well with the given μ_a within 6% error. Through this experimental analysis, the effectiveness of the proposed technique was verified.

Table 2. Results of absorption coefficient estimation.

Given μ_a [/mm]	Estimated μ_a [/mm]	μ_a Estimation error [%]
0.010	0.0103	3.0
0.0075	0.0072	4.0
0.0050	0.0053	6.0

IV. Depth Estimation with Unknown Medium

In the previous chapter, the calibration curves were generated assuming that one of the optical parameters is known. To make the proposed technique more useful in practice, we modify it to be applicable to the case when both the optical parameters (μ_s' and μ_a) are unknown. In the diffusion equation that describes the light propagation in a turbid medium, the attenuation coefficient of light intensity is described in terms of the effective attenuation coefficient $\mu_{eff} = \sqrt{3\mu_a(\mu_s' + \mu_a)}$ [4]. Therefore, we modified the proposed technique to generate the calibration curves as a function of μ_{eff} instead of μ_s' and μ_a. In this way, the two independent parameters μ_s' and μ_a are combined into one new parameter μ_{eff}. Thus, we can apply the proposed technique to the case when both μ_s' and μ_a are unknown.

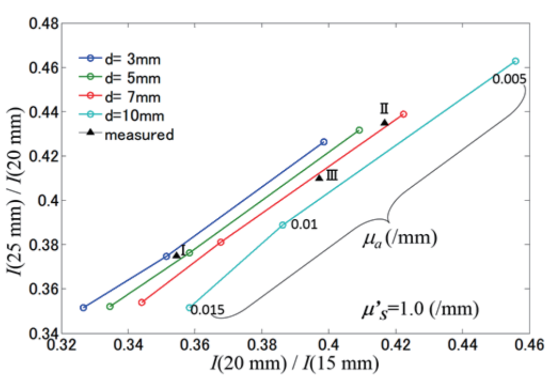

Figure 5. Calibration curves obtained in experiment with fixed μ_s'.

Fig. 6 shows the calibration curves generated in the experiment described in section III.C. The result of the depth and μ_{eff} estimation for the cases I and II were summarized in Table 3. The μ_{eff} of the case I was calculated from μ_s'= 1.0 /mm and μ_a=0.005 /mm of the turbid medium. The μ_{eff} of the case II was calculated from μ_s'= 1.0 /mm and μ_a=0.01 /mm of the turbid medium. The good agreement between the estimated and the given values was confirmed both in the depth and μ_{eff}.

Table 3. Results of depth estimation with known optical paremeters.

Case	Given depth [mm]	Estimated depth [mm]	Estimation error [%]
I	5.0	5.13	2.6
II	7.0	8.03	14.7
	Given μ_{eff} [/mm]	Estimated μ_{eff} [/mm]	Estimation error [%]
I	0.123	0.126	2.4
II	0.174	0.180	3.4

V. Estimation of All Parameters

Next, we attempted to apply the proposed technique to estimate all the three parameters. It can be realized in the following iterative and convergent processes. In this technique, μ_a and μ_s' are alternately estimated switching the calibration curves with a single unknown optical parameter such as Fig. 3(a) or 3(b). Repeating these processes, converged μ_a and μ_s' can be obtained.

(1) Obtain calibration curves as a function of μ_a such as Fig. 3(a) with a fixed μ_s' in a computer simulation or a phantom measurement. Repeat this process for conceivable different values of μ_s'. Name this series of calibration curves Group A.

(2) Obtain calibration curves as a function of μ_s' such as Fig. 3(b) with a fixed μ_a in a computer simulation or a phantom measurement. Repeat this process for conceivable different values of μ_a. Name this series of calibration curves Group B.

Measure the fluorescent intensities I_L, I_M and I_S at the body surface for the excitation light sources at large,

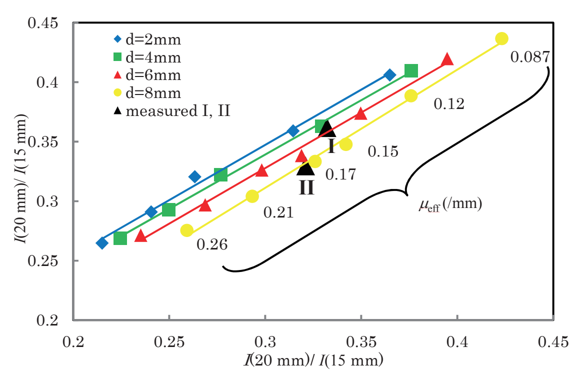

Figure 6. Calibration curves obtained in experiment for simultaneous estimation of object depth and μ_{eff} of turbid medium.

(3) medium and small distances, respectively. Calculate the ratios I_L/I_M and I_M/I_S.
(4) Set the initial value of μ_s' as a typical value, such as 1 /mm. Choose the calibration curves of μ_s'=1 /mm from Group A. Estimate the depth and the μ_a by plotting the point $(x, y) = (I_M/I_S, I_L/I_M)$ in the plane of the calibration curve as explained in the section III.A.
(5) Using the estimated value of μ_a, choose the appropriate calibration curves from Group B. Estimate the depth and μ_s' by plotting the point $(I_M/I_S, I_L/I_M)$ in the plane of calibration curves.
(6) Using the estimated value of μ_s', choose the appropriate calibration curves from Group A. Estimate the depth and μ_a.
(7) Repeat the processes (5) and (6) until the estimated depth converges into a preset fluctuation threshold.
(8) The μ_a and μ_s' in the final process are the values to be estimated.

The convergence of these processes was confirmed in computer simulation and experiments. Two of the experimental results are presented in Table 4. The estimated values agreed with the given values with the maximum error of 40%. The numbers of iteration to obtain this data were 68 and 40 for case I (5 mm depth) and case II (7 mm depth), respectively. Through this analysis, we could confirm the feasibility of the proposed technique to estimate the depth in the scattering medium with unknown μ_a and μ_s'.

Table 4. Results of optical constants estimation.

Case	Given optical constants (μ_s' and μ_a) [/mm]	Estimated optical constants [/mm]
I	1.0, 0.005	0.84, 0.0070
II	1.0, 0.010	1.24, 0.0091

VI. Improvement of TFI

Finally the effectiveness of the proposed technique to improve the image obtained in TFI was examined in experiment. Fig. 7(a) shows the image of the fluorescent object in clear water using the experimental setup described in section III.B. The left images of Figs. 7(b) and 7(c) are the observed images of the case I and II as described in previous chapter (I: μ_s'= 1.0 /mm, μ_a = 0.005 /mm, d=5mm and II: μ_s'= 1.0 /mm, μ_a = 0.010 /mm, d=7 mm), respectively. As the fluorescent object became deeper, the image became more blurred and indistinct. Using the estimated values of the depth (Table 3) and optical parameters (Table 4), the PSF was calculated according to the reference [2]. The right images of Figs. 7(b) and 7(c) are the results of the deconvolution with the PSF.

The square-shape is not perfectly recovered. However, the true size of the fluorescent object was almost retrieved. Moreover, we have tested chicken meat instead of the Intralipid suspension for turbid media, and the validity of the proposed technique was confirmed with the animal meat, as well.

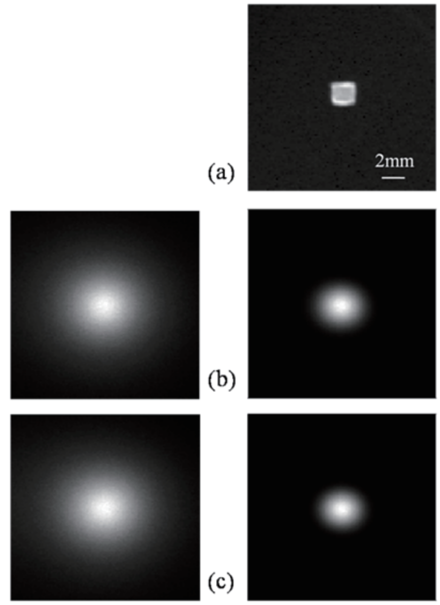

Figure 7. Result of image improvement (a) image in clear water, (b) observed (left) and improved (right) images for 5 mm depth, and (c) observed (left) and improved (right) images for 7 mm depth.

VII. Conclusion

To improve the image of a fluorescent object in TFI, the PSF deconvolution is an effective method. The depth of the fluorescent source is an essential and important parameter to obtain an accurate PSF. A technique was developed to estimate the depth of a fluorescent source in a turbid medium. We can estimate the depth from the fluorescent intensity measured at the body surface using multiple emitters at different distances. If one of the optical parameters, μ_s' or μ_a is known, the depth and another unknown optical parameter can be estimated at the same time. The technique was modified so that we can estimate all the three parameters, i.e. the depth, μ_s' and μ_a at the same time. The feasibility of these techniques was confirmed in computer simulation and experiment. The effectiveness of the proposed technique was verified in the improvement of the images of TFI.

The proposed technique is effective for the fluorescent objects that are separately observable at the body surface. Further study is required to apply the proposed technique to the fluorescent objects widely distributed in different depths

References

[1] M. V. Marshall, J. C. Rasmussen, I.-C. Tan, M. B. Aldrich, K. E. Adams, X. Wang, C. E. Fife, E. A. Maus, L. A. Smith, and E. M. Sevick-Muraca, "Near-Infrared Fluorescence Imaging in Humans with Indocyanine Green: A Review and Update," *Open Surg Oncol J.*, vol. 2, no. 2, pp. 12–25, May 2010.
[2] K. Shimizu, K. Tochio, and Y. kato, "Improvement of transcutaneous fluorescent images with a depth-dependent point-spread function," *Appl. Opt.*, vol. 44, no. 11, pp. 2154–2161, Apr. 2005.
[3] A. Shimizu, Y. Kato, and K. Shimizu, "Depth estimation and image improvement of fluorescent objects in scattering medium by reflection-type measurement with two light sources," *IEICE. Tech. Rep.*, vol. 109, no. 460, pp. 133–138, Mar. 2010 (*in Japanese*).
[4] A. Ishimaru, "Wave propagation and Scattering in Random Media," *Academic Press*, 1977.